MEDIA SuUB Bremen
https://media.suub.uni-bremen.de

Titel/Title: Partitioning of primary shear zone heat in face milling

Autor*innen/Author(s): Langenhorst, L., Sölter, J., Heinzel, C.

Veröffentlichungsversion/Published version: Postprint

Publikationsform/Type of publication: Artikel/Aufsatz

Empfohlene Zitierung/Recommended citation:

L. Langenhorst, J. Sölter, C. Heinzel, Partitioning of primary shear zone heat in face milling, CIRP Annals, Volume 71, Issue 1, 2022, Pages 53-56, ISSN 0007-8506, https://doi.org/10.1016/j.cirp.2022.04.010.

Verfügbar unter/Available at:
(wenn vorhanden, bitte den DOI angeben/please provide the DOI if available)

https://doi.org/10.1016/j.cirp.2022.04.010.

Zusätzliche Informationen/Additional information:

(https://www.sciencedirect.com/science/article/pii/S0007850622000506)
Abstract: The outcome of this paper allows calculating the fraction of heat generated in the primary shear zone that is transferred to the workpiece in face milling. The proposed approach is based on a sequentially coupled analysis of the heat partitioning in the cutting edge normal plane and in the reference plane. The latter, for the first time, allows to

Partitioning of primary shear zone heat in face milling

Langenhorst, L. [b], Sölter, J. [a,b], Heinzel, C. (2) *[a,b]

[a] University of Bremen, MAPEX Center for Materials and Processes, Faculty of Production Engineering, Dept. of Manufacturing Processes, Bremen, Germany
[b] Leibniz Institute for Materials Engineering, Dept. of Manufacturing Technologies, Badgasteiner Str. 1-3, D-28359 Bremen, Germany

The outcome of this paper allows calculating the fraction of heat generated in the primary shear zone that is transferred to the workpiece in face milling. The propo ed approach is based on a sequentially coupled analy is of the heat partitioning in the cutting edge normal plane and in the reference plane. The latter, for the first time, allows to systematically take into account the removal of heated workpiece material by subsequent cutting tool engagements. The generated heat is related to the uncut chip thickne . Utilizing Weiner's approach, the heat flux density distribution is determined which serves as input for a three-dimensional thermal finite element simulation that is validated experimentally by temperature measurements.

Keywords: Milling, Simulation, Heat Partitioning

1. Introduction and state of the art

Regarding the functional performance of manufactured parts, the effects caused by the heat transferred to the workpiece during machining is of significant importance. Dimensional and form deviations are influenced by the thermal impact which might also impair the surface layer properties by the generation of tensile residual stresses or the initiation of phase transformations. If tool wear is neglected, the heat generated in the primary shear zone is the main cause for the thermal impact on the workpiece in metal cutting. Its partitioning is solely driven by solid state convection due to the material flow and the diffusion of heat.

Komanduri and Hou discussed analytical models for orthogonal cutting developed since the 1950s to determine the heat partitioning and extended an approach presented by Hahn [1] to calculate steady-state temperature fields in the chip and workpiece [2]. For different materials and cutting conditions in orthogonal cutting, Komanduri and Hou confirmed the dependence of the heat partition in the primary shear zone on the thermal number $N_{th,n} = h \cdot v_c \cdot a^{-1}$, where h is the uncut chip thickness, v_c the cutting speed and a the temperature diffusivity of the workpiece material, already formulated by Chao and Trigger [3]. Similar correlations were also found by numerical models, e.g. by means of chip formation simulations by Puls et al. [4]. A closed-form equation for the partitioning of heat generated in the primary shear zone has been developed by Weiner [5]. Recently, a comprehensive study on heat partitioning was carried out by Augspurger et al. [6]. By means of measured temperature fields in the workpiece, the dependence on the thermal number was again confirmed for four different metals.

However, the approaches developed for orthogonal cutting can only be used to a limited extent for cutting processes such as milling, drilling, and turning, since generally an additional feed motion is superimposed on the motion in cutting direction. This essentially leads to a removal of material heated during previous cutting tool engagements, which affects the heat partitioning. This is also indicated by an investigation in which the fraction of heat transferred to the workpiece has been analyzed for different processes and was plotted against $N_{th,n}$ [7]. Qualitatively, the results also show a strong increase in the heat partition with decreasing $N_{th,n}$, but the process-specific deviations are significant. In particular, the influences of the different depths of cut a_p and feed velocities v_f were not taken into account explicitly.

Until today, mainly empirical models have been developed to determine the heat partition or the heat flux into the workpiece for cutting processes, which only allow a limited transferability of the findings to other process conditions. Arrazola et al. give a broad overview on modelling approaches [8]. Based on temperature measurements before and after the process, Fleischer et al. [9] and Denkena et al. [10] determine the heat partition in milling and drilling. Utilizing an iterative adaption of simulated temperature fields to measurements, Segurajauregui and Arrazola [11] determine the heat partition in drilling. Similarly, Biermann et al. [12] follow this approach for deep drilling and Schweinoch et al. [13] as well as one of the authors for milling [14]. It can be summarized that the influence of the chip removal due to the feed velocity on heat partitioning is not taken into account explicitly in these works. Approaches to this can be found in part in Putz et al. [15] for peripheral milling. However, findings are only available for two cutting speeds, according to which a higher cutting speed leads to a lower heat transfer into the workpiece. Functional dependencies of the heat partitioning on the depth of cut and the feed velocity in addition to the uncut chip thickness, the cutting speed, and the temperature diffusivity are needed for practical cutting processes. In the present work, a new approach is introduced that allows to derive these functional dependencies and is validated for face milling.

2. Objective and theoretical approach

The objective of the present work was to find a functional relationship for the fraction of heat generated in the primary shear zone that is transferred to the workpiece. Compared to already published approaches it was the special aim to take into account the removal of preheated workpiece material explicitly and thus the effect of the depth of cut and the feed velocity. The approach is based on the assumption that the heat partitioning in the primary shear zone can be subdivided into a sequentially coupled heat partitioning in (1) the cutting edge normal plane and in (2) the reference plane (Fig. 1). The first model describes the heat partitioning between the chip and the workpiece material for orthogonal cutting conditions. The latter allows to

systematically take into account the partial removal of heated workpiece material by cutting tool engagements due to the tool feed without the need to simulate the chip formation in detail. From a kinematic model, the distribution of the uncut chip thickness h at the tool-workpiece contact surface (cutting arc) A is calculated. The local heat partition to the workpiece R_n in the cutting edge normal plane is calculated based on orthogonal cutting models (model 1). Moreover, it is assumed that the generated heat is related to the uncut chip thickness h, which enables the calculation of a heat flux density distribution, which is used as an input in a three-dimensional thermal finite element simulation (model 2). By utilizing the heat flux density distribution, the total heat partition to the workpiece R_{total} is calculated from a temperature increase in the cross sectional surface B.

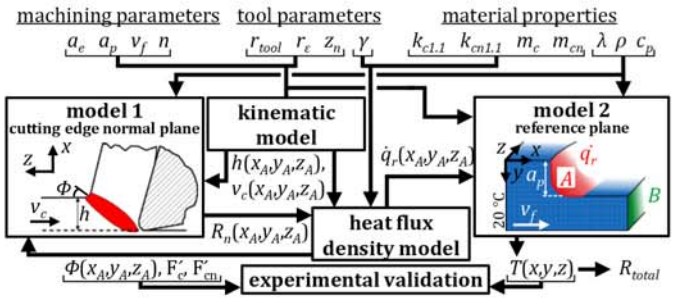

Fig. 1. Modelling approach for the calculation of three-dimensional heat partitioning in face milling.

Analogously to the thermal number $N_{th.n}$ that describes the heat partitioning in the primary shear zone in orthogonal cutting, in this work, the heat partitioning in the reference plane shall be described by the dimensionless thermal number $N_{th.r} = a_p \cdot v_f \cdot a^{-1}$.

Finally, a functional relation between the simulated total heat partition R_{total} and both dimensionless thermal numbers is developed. Simulated heat partitions were validated by simulated and measured temperatures in face milling.

3. Experimental procedure

A vertical machining center Deckel Maho, type DMC 65V, was used for the experimental investigations on dry face milling. The workpieces had dimensions of 80 x 40 x 10 mm³ and consisted predominantly of the normalized steel 42CrMo4 (AISI 4140). In addition, the aluminum alloy AlZnMgCu1.5 (A97075) was also investigated to clarify to what extent the thermal diffusivity a sufficiently takes into account the material behavior. The experimental setup is shown in Fig. 2a. The tools used were single-edged cemented carbide milling cutters, in order to have a constant cutting geometry throughout the process and to keep the cutting geometry simple (compared to complex indexable inserts) for the modelling. A full factorial 3^3 experimental design was conducted with 3 realizations, varying v_c, v_f, and a_p according to Fig. 2b. In order to exclude the influence of tool wear as far as possible, the tools were changed after 9 trials.

(b)
tool parameters
D_{tool} = 10 mm, κ = 90°, z = 1
r_ε = 0.2 mm, r_β = 2 µm, γ = 0°
workpiece material
42CrMo4 (AISI 4140), 211 HV1
AlZnMgCu1.5 (A97075), 185 HV1
machining parameters
a_p = [0.5, 1.0, 1.5] mm
v_c = [150, 250, 350] m/min
v_f = [250, 450, 650] mm/min
→ f_z = 45...272 µm

Fig. 2. Experimental setup including force and temperature measurement (a) as well as varied and constant experimental parameters (b).

The small workpiece width, the centered tool (first up then down milling), and the resulting small differences in uncut chip thickness over surface A allow to calculate the shear angle Φ by means of measured chip length, width, and weight, cf. [16], p. 20.

The temperature field was measured on the workpiece surface (cf. Fig. 1, xy-plane at z = 0) with the ImageIR 8300 thermographic camera from InfraTec using a microscope lens (magnification M = 1, working distance WD = 200 mm) with an integration time of 500 µs. The experimental setup allowed to follow the feed movement of the tool and was thus able to record a quasi-stationary temperature field in the area of the tool engagement. Via a trigger, the camera took one image per tool rotation. The samples were painted matt black. To calibrate the thermographic camera, samples were prepared with heating cartridges and heated to defined temperatures (20 - 120 °C in 5 °C-steps). With the signal of a thermocouple welded onto the measuring surface, calibration curves were created for both materials.

4. Simulation and validation

4.1. Kinematic model and heat partitioning model in the cutting edge normal plane (model 1)

The kinematic model was used to determine the local uncut chip thicknesses h and the local cutting speeds v_c, whereby a sufficiently accurate approximation of the uncut chip thicknesses in face milling can be made by the shortest distance between two tool envelope surfaces displaced by the feed per tooth f_z, taking the corner radius r_ε into account (refer to Fig. 4 in [17]).

The model in the cutting edge normal plane describes the local partition of the heat generated in the primary shear zone between the workpiece and the chip for each FE-node in the reference plane model. In [18], the results of orthogonal cutting models describing the heat partition as a function of the thermal number $N_{th.n}$ were compared, investigated, and evaluated with respect to further influencing factors. It was shown that the closed-form solution of the fraction of shear plane heat transferred to the workpiece according to Weiner $\beta(\sqrt{Y_L})$, with $Y_L = 0.25 \cdot N_{th.n} \cdot \tan(\Phi)$, β denoted here as R_n [5], leads to almost identical results compared to the more computationally demanding model from Komanduri and Hou [2]. Temperature-dependent thermo-physical properties were taken from [19].

4.2. Heat flux density model and heat partitioning model in the reference plane (model 2)

The reference plane model was set up as a three-dimensional steady-state heat transfer problem in the FEM-software Abaqus to solve the forced convection-diffusion equation. The mass flow rate is defined by the material density ρ and the feed velocity v_f. Material that has not yet been heated is modelled by a 20 °C boundary condition at one edge. The model boundaries are otherwise defined as adiabatic (except the heat input at surface A) and as free with respect to convection in the feed direction. Both, the heat flux through surface B (heat flux in the remaining workpiece P_{wp}) and in the removed undeformed chip volume at the engagement surface A (heat flux into subsequent chips P_A - P_{wp}) as well as the heat input via the heat flux density $\dot{q}_r$ are considered stationary due to the high cutting engagement frequency. As a result, the reference plane model provides a quasi-stationary temperature field $T(x,y,z)$.

In the heat flux density model, for the determination of the shear power density, it is taken into account that the heat input is not discrete in time, but that the work W_A performed during the time of a cutting action t_e is continuously dissipated (cf. Eq. 1).

$$W_A = \int_0^{t_e} P_{shear} \cdot R_n \, dt = t_e \cdot \int \dot{q}_r \, dA = t_e \cdot \int \dot{q}_s \cdot R_n \, dA \qquad (1)$$

The product of local shear power density $\dot{q}_s(x_A,y_A,z_A)$ and local heat partition $R_n(x_A,y_A,z_A)$ is transferred to the reference plane

model as the heat flux density $\dot{q}_r(x_A,y_A,z_A)$. For each FE-node, orthogonal cutting conditions are assumed locally. To determine the local shear power P_{shear}, the shear plane model according to Ernst and Merchant is used to obtain functional relationships for the shear angle, cf. [16], p. 128, the friction angle and shear force, cf. [16], p. 18, as well as the shear speed, cf. [16], p. 24. For the calculation of the friction angle and the shear force, local cutting force F_c as well as local cutting normal force F_{cn} are calculated according to the force model from Kienzle depending on the local uncut chip thickness h and material-specific parameters [20].

On average over all tests, the relative deviation between calculated cutting forces for $h = f_z$ and mean values of the measurement is 8.7 %. Regarding the shear angle, the measurements of the chips reveal an average relative deviation of 11.6 %, which is acceptable considering the small chips in interrupted cutting.

4.3. Comparison of measured and simulated process temperatures

From the calibrated thermographic images, the difference between the initial workpiece temperature and the temperature of each pixel (17 x 17 µm² in size) averaged over up to 200 images recorded during machining was determined and again averaged for the three repetitions. The small differences between the individual images confirm the quasi-stationary character of the measured temperature fields. Fig. 3 shows the graphical comparison of simulated and measured process-related temperature rises for an exemplary and representative test. The high level of agreement, not only for specific points but also for the entire temperature field, is an indication for the validity of the chosen modelling approach. This is especially true because no inverse modelling and iterative adjustment was carried out, in contrast to comparable works in literature.

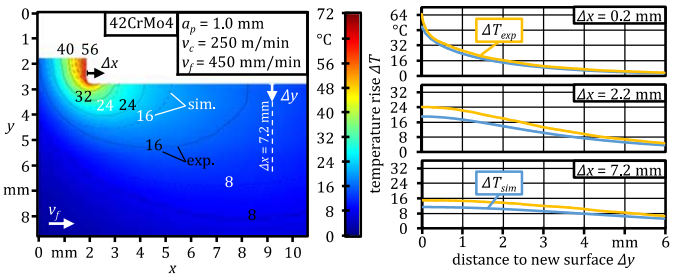

Fig. 3. Comparison of measured and simulated (a) isotherms and (b) temperature depth profiles at three distances to the cutting arc Δx.

In order to obtain a quantitative statement on the validity for all tests with regard to heat partitioning, specific heat fluxes $P_{wp}/\Delta z$ transferred through three vertical lines at Δx = 0.2, 2.2, and 7.2 mm were calculated based on measured and simulated temperature profiles according to Eq. 2.

$$P_{wp} = c_v \cdot \rho \cdot v_f \cdot \sum \Delta T(x,y,z) \cdot \Delta y \cdot \Delta z \qquad (2)$$

In the following figures, a relative deviation of one or more of these three heat fluxes below an arbitrarily chosen value of 15 % is indicated by green filled dots. For the temperature profiles shown above, the deviations of heat fluxes are 13.3 % (Δx = 0.2 mm), 22.9 % (Δx = 2.2 mm), and 24.2 % (Δx = 7.2 mm) and thus the validity was proven for one line.

5. Heat partitioning in face milling

The total heat partition R_{total} describes the fraction of shear zone heat that is transferred into the workpiece and not being removed by subsequent cutting edge engagements. Accordingly, this fraction is determined by the heat flux $P_{A,Rn=1}$ into the surface A due to the shear power and the heat flux P_{wp} transferred into the final workpiece. Eq. 3 shows this relation and its calculation by multiplying the cutting edge normal plane heat partition to the workpiece $R_{n.r}$ and the reference plane heat partition to the workpiece R_r. The heat flux P_{wp} is calculated by Eq. 2 using the simulated temperatures at surface B. The heat flux P_A can be determined numerically by an adjusted transient reference plane model, in which the equilibrium temperature in an adiabatic workpiece is simulated after the heat source has been active for a certain while. Without additional numerical simulation, the heat flux can equally be obtained by integrating the heat flux density over the surface A. In order to determine the heat flux due to shear power $P_{A,Rn=1}$, the local heat partition R_n in Eq. 1 is set to be one. Otherwise, to determine the heat flux $P_{A,Rn\neq1}$, which is already reduced by the heat flux transferred into the chip in the cutting edge normal plane, the local heat partition R_n according to Weiner has to be considered.

$$R_{total} = \frac{P_{wp}}{P_{A,Rn=1}} = \frac{P_{A,Rn\neq1}}{P_{A,Rn=1}} \cdot \frac{P_{wp}}{P_{A,Rn\neq1}} = R_{n.r} \cdot R_r \qquad (3)$$

The cutting edge normal plane heat partition $R_{n.r} = P_{A,Rn\neq1} / P_{A,Rn=1}$ as the fraction of shear zone heat transferred into the workpiece according to local calculations is shown in Fig. 4. The simulation results agree very well with Weiner's function for R_n if the local uncut chip thickness h is substituted by the averaged uncut chip thickness $\bar{h}$ over the surface A (black line). Temperature measurements validate this for steel over a wide area of the experimental design. Also shown are simulation results where the shear angle has been varied within the scatter limits determined from the chip measurements. The heat partition increases with a decreasing shear angle and due to the consideration of the shear angle in the dimensionless number there is still a clear correlation.

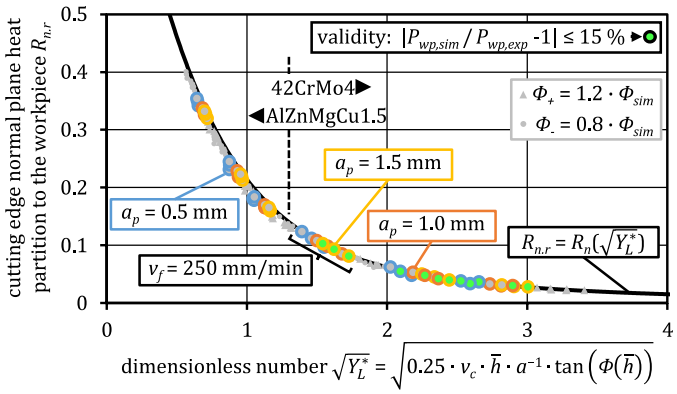

Fig. 4. Heat partitioning in the cutting edge normal plane.

In analogy to the dimensionless number for the cutting edge normal plane, the reference plane heat partition R_r in Fig. 5 is plotted over the dimensionless number $N_{th.r}$. In the reference plane, heat transfer by solid state convection is caused by the feed velocity v_f (instead of the cutting speed v_c), and the distance from the initial to the newly generated workpiece surface is the depth of cut a_p (instead of the uncut chip thickness h), cf. Fig. 1. In this analogy the shear angle corresponds to the major cutting edge angle, which is $\kappa = 90°$ neglecting the corner radius. An increasing dimensionless number $N_{th.r}$ in the reference plane also results in a lower reference plane heat partition R_r and thus in a lower fraction of heat flux being transferred into the workpiece without being removed by subsequent cutting edge engagements. Furthermore, this is essentially independent of the cutting speed, varied shear angles, and magnitude of applied heat flux. For further investigation of the correlation and the analogy to the cutting edge normal plane, heat partitions calculated by means of temperature simulations according to an orthogonal cutting model are also plotted (red diamonds). Since Weiner's differential equation fails to account for an angle $\Phi = 90°$, the model from Komanduri and Hou was used instead. Despite the two-

dimensional approach of a semi-infinite body and no consideration of the tool corner radius and varying uncut chip thickness, the results are very similar to the values of the heat partition model and follow the specified exponential regression function (black line).

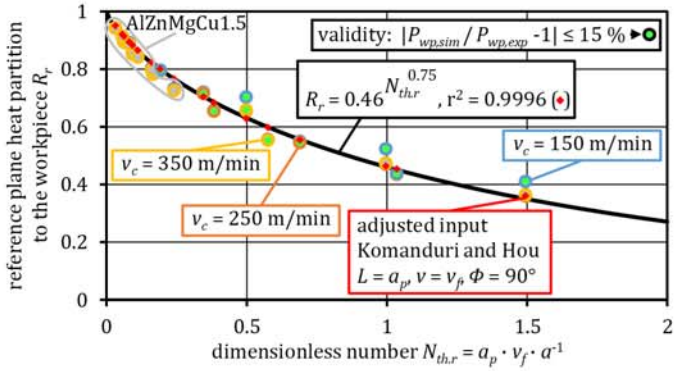

Fig. 5. Heat partitioning in the reference plane.

For the validated tests, the separation of heat transfer phenomena during face milling in two planes is feasible, and for both, the cutting edge normal plane and the reference plane, the heat partition can be approximated by corresponding functions depending on a dimensionless number. The total heat partition R_{total} thus also depends on the two dimensionless numbers and can be plotted as a three-dimensional diagram (Fig. 6). The results of the heat partition model fit very well to the product of $R_n(\sqrt{Y_L^*})$ and the exponential function and, in case of steel, are validated over a wide range. The residuals plotted in red increase with decreasing dimensionless numbers and therefore show higher differences for the aluminum, which is also indicated by the coefficient of determination r^2.

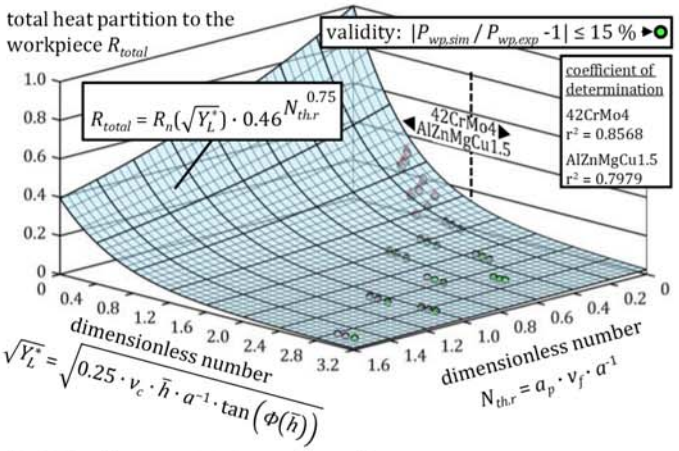

Fig. 6. Total heat partitioning in face milling.

6. Conclusions

The presented approach allows to simulate the total heat partition R_{total} in metal cutting processes that means the fraction of shear plane heat transferred to the workpiece taking into account the removal of heated workpiece material. This approach goes beyond the simplification of an orthogonal cutting process as it takes into account the depth of cut and the feed velocity. The functional dependency of the total heat partition R_{total} on two dimensionless numbers, comprising uncut chip thickness, cutting speed, depth of cut, feed velocity, and temperature diffusivity, is shown for a face milling process.

The fundamental procedure of the presented approach is to decompose the total heat partitioning into a sequentially coupled heat partitioning in the cutting edge normal plane (1) and the reference plane (2). The comparison of simulation results with measurements in face milling shows a good agreement for the 42CrMo4 steel whereas differences are observed for the aluminum alloy AlCuZnMg1.5. From these results, it is concluded that the proposed approach is valid as long as the thermal diffusivity of the workpiece material is comparatively low (42CrMo4: $a \approx 10.9$ mm²/s; AlZnMgCu1.5: $a \approx 67.5$ mm²/s). In this case, the assumption of a stationary heat flux density in the reference plane seems to be valid. The proposed approach allows to calculate the functional relationship between heat partition in face milling and two dimensionless numbers $\sqrt{Y_L^*}$ and $N_{th,r}$ (Fig. 6).

Acknowledgements

The authors thank the Deutsche Forschungsgemeinschaft (DFG) for funding this work within the research project "Model-based Determination of Heat Partitioning in Industry Relevant Dry Cutting Processes" – Project number 389472108.

References

[1] Hahn R S (1951) On the temperature developed at the shear plane in the metal cutting process. Proceeding of the First US National Congress of Applied Mechanics:661–666.

[2] Komanduri R, Hou Z B (2000) Thermal modeling of the metal cutting process Part I - Temperature rise distribution due to shear plane heat source. Int J Mech Sci 42:1715–1752.

[3] Chao B T, Trigger K J (1953) The significance of thermal number in metal machining. Transactions of ASME 75:109–120.

[4] Puls H, Klocke F, Veselovac D (2016) FEM-based prediction of heat partition in dry metal cutting of AISI 1045. Int J Adv Manuf Technol 86:737–745.

[5] Weiner J H (1955) Shear-Plane Temperature Distribution in Orthogonal Cutting. Transactions of ASME 77:1331–1341.

[6] Augspurger T, Bergs T, Döbbeler B (2019) Measurement and Modeling of Heat Partitions and Temperature Fields in the Workpiece for Cutting Inconel 718, AISI 1045, Ti6Al4V, and AlMgSi0.5. J Manuf Sci Eng 141:61007.

[7] Sölter J, Frohmüller R, Wirbser H (2018) Temperature measurements and heat partitioning in machining processes. In: Thermal Effects in Complex Machining Processes: Lecture Notes in Production Engineering. Eds. Biermann D, Hollmann F. Springer:5–21.

[8] Arrazola P J, Özel T, Umbrello D, Davies M, Jawahir I S (2013) Recent advances in modelling of metal machining processes. CIRP Ann Manuf Techn 62/2:695–718.

[9] Fleischer J, Pabst R, Kelemen S (2007) Heat Flow Simulation for Dry Machining of Power Train Castings. CIRP Ann Manuf Techn 56/1:117–122.

[10] Denkena B, Maaß P, Schmidt A, Niederwestberg D, Vehmeyer J, Niebuhr C, Gralla, P (2018) Thermomechanical Deformation of Complex Workpieces in Milling and Drilling Processes. In: Thermal Effects in Complex Machining Processes: Lecture Notes in Production Engineering. Eds. Biermann D, Hollmann F. Springer:219–250.

[11] Segurajauregui U, Arrazola P J (2015) Heat-flow determination through inverse identification in drilling of aluminium workpieces with MQL. Prod. Eng. Res. Devel. 9:517–526.

[12] Biermann D, Blum H, Iovkov I, Rademacher A, Rosin K, Suttmeier F-T (2018) Modeling, Simulation and Compensation of Thermomechanically Induced Deviations in Deep-Hole Drilling with Minimum Quantity Lubrication. In: Thermal Effects in Complex Machining Processes: Lecture Notes in Production Engineering. Eds. Biermann D, Hollmann F. Springer:181–218.

[13] Schweinoch M, Joliet R, Kersting P, Zabel A (2015) Heat input modeling and calibration in dry NC-milling processes. Prod. Eng. Res. Devel. 9:495–504.

[14] Sölter J, Gulpak M (2012) Heat partitioning in dry milling of steel. CIRP Ann Manuf Techn 61/1:87–90.

[15] Putz M, Oppermann C, Semmler U, Bräunig M, Karagüzel U (2017) Consistent Simulation Strategy for Heat Sources and Fluxes in Milling. Procedia CIRP 62:239–244.

[16] Shaw M C (2005) Metal Cutting Principles, 2nd Ed. Oxford University Press.

[17] Langenhorst L, Cihan M, Sölter J (2019) A Three Dimensional Calculation Approach for the Heat Flux Density Distribution in Face Milling. Procedia CIRP 82:8–13.

[18] Langenhorst L, Sölter J, Kuschel S (2020) Partition of Primary Shear Plane Heat in Orthogonal Metal Cutting. J Manuf Mater Process 4/3:82.

[19] Spittel M, Spittel T, Warlimont H, Landolt H, Börnstein R, Martienssen W (2011) Numerical data and functional relationships in science and technology. Springer: Landolt-Börnstein Group VIII Advanced Materials and Technologies.

[20] König W, Essel K (1973) Specific Cutting Force Data for Metal-Cutting. Stahleisen Düsseldorf.